

A marine thruster's model identification based on experimental-simulation approach

Abdelmalek Laidani, Mohamed Bouhamida, Zakaria Bellahcene

AVCIS Research Laboratory, Department of Automatics, Faculty of Electrical Engineering,
University of Sciences and Technology of Oran (USTO), Algeria

Article Info

Article history:

Received Dec 27, 2021

Revised Jun 4, 2022

Accepted Jul 22, 2022

Keywords:

Hybrid identification

Low-cost test bench

Marine thruster

ROS toolbox

Underwater vehicle

UUV simulator

ABSTRACT

In recent years, underwater vehicles play a very important role in the marine field, and tasks cannot be accomplished quickly and accurately without the use of such devices. Despite the progress achieved, these vehicles still have problems with their controls in order to have a very good dynamic positioning or a path tracking accurately, and these problems have a direct link to their thrusters, either by negligence or by ignorance of its mathematical model. Several works were carried out to have an accurate model of them, but its behavior is still difficult to be described and it strongly influences the behavior of a vehicle in which it is integrated. In this work we try to deal this problem in the aim to identify a marine thruster designed by us using a low-cost test bench and a hybrid identification approach, which combines the both experimental and simulation parts. The thruster will be integrated on a remotely operated vehicle under development by AVCIS-Lab to make simulation using unmanned underwater vehicle (UUV) simulator and robot operating system (ROS) toolbox under MATLAB. The outcomes will be presented at the end of this paper.

This is an open access article under the [CC BY-SA](#) license.



Corresponding Author:

Abdelmalek Laidani

AVCIS Research Laboratory, Department of Automatics, Faculty of Electrical Engineering

University of Sciences and Technology of Oran (USTO)

Oran, Algeria

Email: abdelmalek.laidani@univ-usto.dz

1. INTRODUCTION

By the growing of the number for commercial, scientific and military applications of underwater vehicles autonomous underwater vehicle/remotely operated vehicle (AUV/ROV), the speed and position control system of them are subject to an increased focus, and to improve their precision, a good control of the force generated by the thruster is necessary [1], [2]. A thruster is the most important actuator in an underwater vehicle [3], built from a motor and a propeller [4], it generates a thrust force allowing the vehicle to move. Thruster control system is situated in the most inner control loop (low level part) [5], and its main purpose is to fulfill the high level control commands from dynamic positioning (DP) system or Joystick [6]. The associated underwater vehicle control system is heavily dependent on the performance and response of this actuator [7], for this reason their characteristics must be modelled accurately [8], [9]. Obtaining the mathematical model of a thruster is more complex because it depends on the model of motor, the propeller and other unknown factors like ambient water speed [10], [11]. The identification is the best way to obtain the model of thruster [12], [13], but it requires an adequate equipment called test bench. A test bench for the identification of marine thrusters is generally constituted by: a tank filled with water, a thruster's carrying structure and instrumentation which

will make it possible to control the thruster and the measurement of the different physical quantities needed [14]. The realization is multidisciplinary because it requires skills in electrical and mechanical engineering. Several laboratories have been interested in the realization of test benches in order to identify their thrusters and a bibliographical analysis made in [15] shows this. The objective of this research is to obtain an accurate dynamic model of marine thruster using a low-cost test bench and a hybrid identification approach, this approach reduce effort in developing complex analytical solution by combining between the simulation parts and the experimental part. The organization of this article will be as follows: we start by focusing on the model of the thruster that we will propose, after we present the methodology of its identification, our approach and the results obtained. The integration of the thruster's model on a ROV under unmanned underwater vehicle (UUV) simulator and using robot operating system (ROS) toolbox will be presented in the final section to show its behaviors. A conclusion and perspectives will be discussed at last.

2. THE THRUSTER'S MODEL

A thruster, as defined previously, is composed of an electrical machine (actuator), a propeller, a transmission shaft and the frame that supports the whole, as shown in the Figure 1. In marine propulsion there are 3 types of electric machines; direct current (DC) motor with brushes, brushless synchronous motor and induction motor [16]. These actuators (motors) require pre-actuators (drivers) to vary their speeds, so it is necessary to act on the pre-actuator which will act on the actuator then the latter will absorb a power to deliver a thrust force or a hydrodynamic torque. In works that deal with the marine propulsion the pre-actuator is not taken into consideration when representing the model of a thruster as shown in the Figure 1(a) although this is the first item to receive the controller's command when we use a digital control. The model of the thruster that we will propose is a model that will take into consideration the pre-actuator. This model will consist of; a pre-actuator, a motor and a propeller as shown in the Figure 1(b).

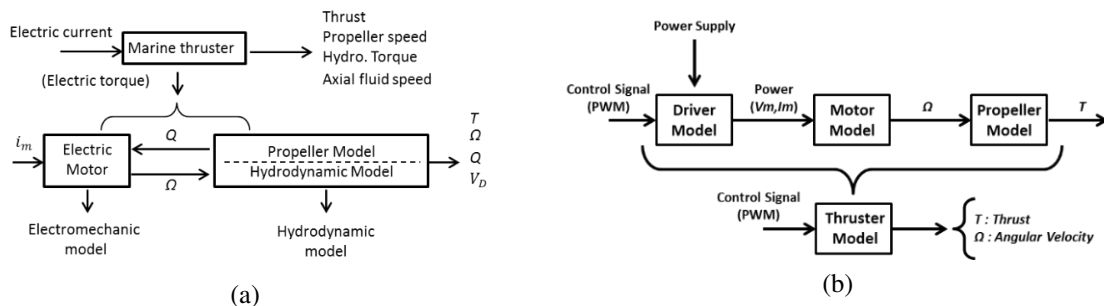


Figure 1. Representation of a thruster model with electric motor for (a) general model [17] and (b) proposed model

The driver (pre-actuator) can be represented as a gain that transforms a pulse width modulation (PWM) input signal (μs) into a voltage supplied for the actuator (motor), its response is linear.

$$Y = a.X + b \tag{1}$$

Where Y represents the output voltage V_m that will be applied to the motor, X the duty cycle of PWM, a and b are constants and given as (by using a power supply of 12 Volts).

$$Y = 0,012.X - 12 \tag{2}$$

For motor modelling there are two approaches; the first is to consider the model of the motor and the propeller as a single model with as input the voltage applied to the motor and the output is the thrust force generated by the propeller, in the second approach both models are considered separately. In our case we will opt for both approaches, the first will be considered in the experimental part with the test bench and the second approach in the simulation part because the model of the brushless direct current motor (BLDC) A2212 that we used in the experimental is already identified in [16] and is in the form of a first order transfer function.

$$G(s) = \frac{\Omega(s)}{V(s)} = \frac{K_m}{1 + \tau.s} \tag{3}$$

With Ω angular velocity of the motor/propeller, V_m is the voltage applied to the motor and :

$$\tau = 0,01021 \text{ s}$$

$$K_m = 131,3016 \frac{\text{rad}}{\text{sec}} \cdot V$$

the Figure 2 shows the response of the motor to a 12 Volts step as an input.

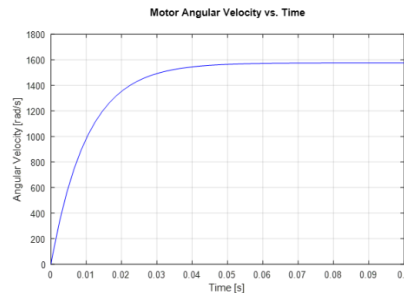


Figure 2. Motor angular velocity response for the input voltage step

The hydrodynamic model (propeller model) used in most scientific works [1], [4], [5], [18], is the steady-state model, this model is simple and was been verified in [19], [20], but there are other models that are more complex and require a lot of measurement to identify their parameters. This model is characterized by a coefficient of thrust noted K_T and a coefficient of the hydrodynamic torque noted K_Q , the block diagram is presented in the Figure 3. The thrust force T and the hydrodynamic torque Q are written in the form of following (4) and (5).

$$T = K_T \cdot \Omega^2 \quad (4)$$

$$Q = K_Q \cdot \Omega^2 \quad (5)$$

In the next section, we looking for determine the coefficients associated with the thrust generated, in order to have a complete thruster model that allows us to do a low level control and integrated it in an underwater vehicle model in the aims to make a high level control such as dynamic positioning or path tracking.

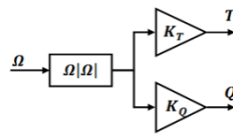


Figure 3. Propeller transfer function block at steady state

3. THRUSTER'S IDENTIFICATION

3.1. Method

The Figure 4 show the equipment and the steps followed for the identification of marine thruster. The method that we implemented is based on the use of the low-cost test bench realized and described in [15] to obtain measurements of the thrust force generated by the thruster (see Figure 4(a)). The method is divided into three steps: the first consists of varying the speed of the thruster gradually from 0 to 100% which corresponds to an PWM from 1000 to 2000 μs and record the data received from the acquisition card, in the second step we make the simulation of the motor model identified in [16] without taking in consideration the hydrodynamic model, in the last step the hydrodynamic model will be deduced from the measurements made and the simulation results obtained. The diagram of the Figure 4(b) shows the steps of the identification method.

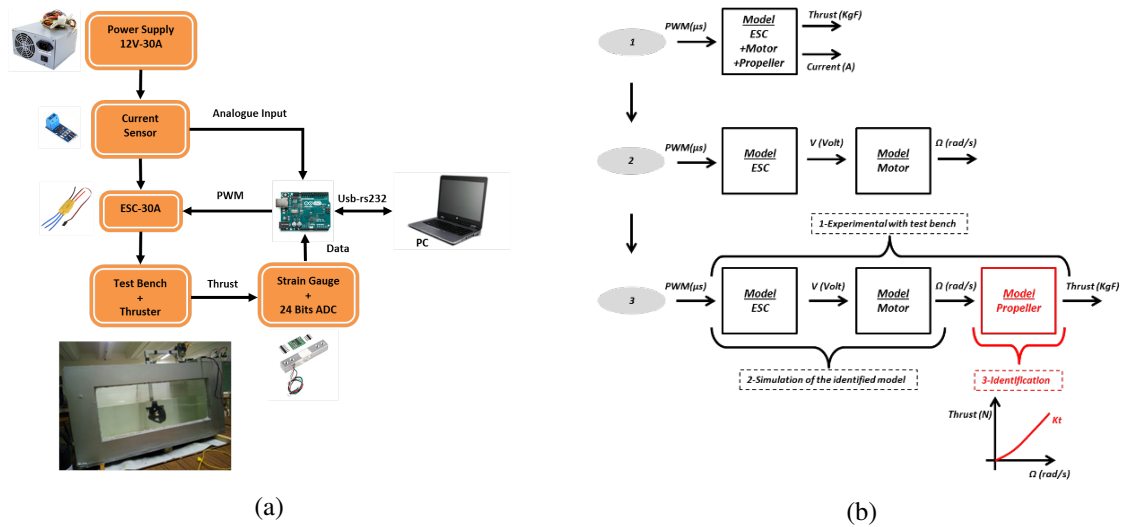


Figure 4. Equipment and method based on for identification: (a) the realized test bench and (b) the steps

3.2. Results

First step: the Figure 5 shows the characteristics of thrust generated by the thruster in both directions (direct as shown in Figure 5(a) and reverse in Figure 5(b)). We notice that there is a dead zone in which the thruster does not respond, it is about $50 \mu s$, then a linear zone is followed which is the operating zone, but from a PWM of $1,800 \mu s$ the thrust force enter in a saturation zone. The thrust force generated in the direct and reverse direction is approximately 1.3 and 1.1 KgF respectively which is equivalent to 12.7 and 10.8 Newton. Second step: the Figure 6 shows the response of the angular velocity vs the PWM input signal, we considered only the linear zone ($PWM \in [1050, 1800]$), because this allows us to obtain a linear relation and simplified the final model. Third step: from the Figure 5 and Figure 6 we can trace the characteristic of the Figure 7 which represents the relationship between the angular velocity and the thrust force generated by the thruster in both directions, see Figure 7(a) for direct direction and Figure 7(b) for reverse direction.

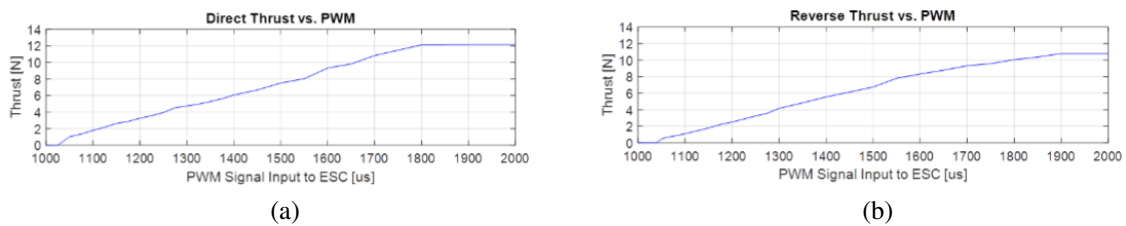


Figure 5. Thrust force generated in (a) direct and (b) reverse direction

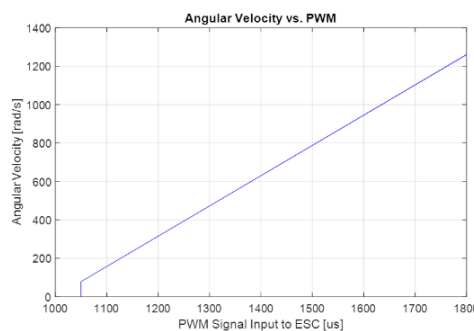


Figure 6. Angular velocity vs. input signal PWM

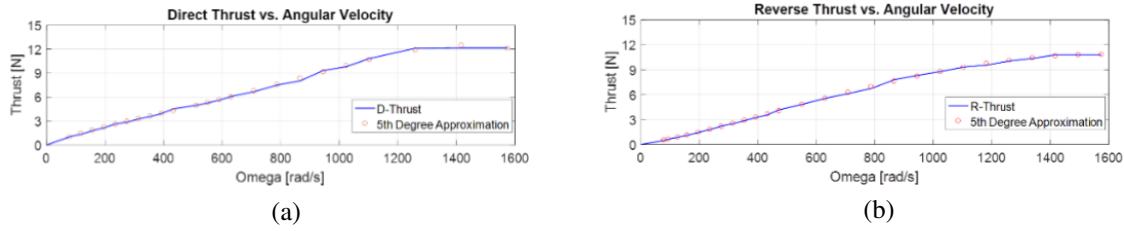


Figure 7. Thrust force vs. angular velocity for (a) direct direction and (b) reverse direction

We notice that there exists a linear relation between force of thrust and angular velocity, this relation can be approximated to a polynomial form as (6).

$$T = K_{T_1}.\Omega^n + K_{T_2}.\Omega^{n-1} + \dots + K_{T_n}.\Omega + K_{T_{n+1}} \quad (6)$$

With K_{T_1} , K_{T_2} , ..., K_{T_n} and $K_{T_{n+1}}$ constants. To correctly choose the degree of the polynomial, we have made the tables below that show the mean error (ME) and the root mean square error (RMSE) between the curve obtained based on the measurements and the polynomials chosen with several degrees, given by the following formulates as (7) and (8).

$$ME = \frac{1}{n} \sum_{i=1}^n |error_i| \quad (7)$$

$$RMSE = \sqrt{\frac{1}{n} \sum_{i=1}^n error_i^2} \quad (8)$$

Table 1 summarize a comparison between the different degrees of the polynomials evaluated for the representation of the propeller model in both direction of thrust, Table 1(a) shown summarize of direct thrust and Table 1(b) shown reverse thrust. This comparison concerns the mean and quadratic errors values of the first 8 polynomials. we notice that as the degree increases, the accuracy increases and the error values decrease. our choice is to take a polynomial of the 5th degree in order to have a relative error of about 1.5% as well as mean and quadratic errors of the order of hundredth of Newton, which will allow us to bring the polynomial closer to the measured values. The constants as mentioned in the (6) for 5th degree polynomial are presented in the Table 2 for direct in Table 2(a) and reverse thrust in Table 2(b) respectively.

The curve of of Figure 7 represents the model of propeller, a 5th degree polynomial approximation is showing also in this figure, and we can notice that the errors are minimum as well as mentioned in the tables previous. Figure 8 represent the global model of the thruster, it consists of two sub models, one for the direct thrust and other for the reverse thrust. Figure 9 shows the blocks under sub models, Figure 9(a) for direct thrust and Figure 9(b) for reverse thrust. each sub model is constituted on the following blocks: electronic speed controller (ESC) model, motor model and propeller model. The switches in the input and the output of the sub model represents the dead and saturation zone respectively.

Table 1. Error comparison for (a) direct thrust and (b) reverse thrust

(a)			(b)		
Order	ME [N]	RMSE [N]	Order	ME [N]	RMSE [N]
1 st	0.3157	0.5162	1 st	0.3793	0.5008
2 nd	0.2552	0.3539	2 nd	0.2306	0.2708
3 rd	0.2170	0.2615	3 rd	0.0706	0.0898
4 th	0.0912	0.1318	4 th	0.0568	0.0822
5 th	0.0935	0.1305	5 th	0.0537	0.0806
6 th	0.0825	0.1088	6 th	0.0538	0.0803
7 th	0.0618	0.0898	7 th	0.0522	0.0758
8 th	0.0603	0.0891	8 th	0.0511	0.0741

Table 2. 5th Degree polynomial coefficients for (a) direct thrust and (b) reverse thrust

(a)		(b)	
Coefficients	Values [$N.s^2.rad^{-2}$]	Coefficients	Values [$N.s^2.rad^{-2}$]
K_{T1D}	$1,3506 * 10^{-15}$	K_{T1R}	$-1.1504 * 10^{-15}$
K_{T2D}	$-1,1879 * 10^{-11}$	K_{T2R}	$5.4431 * 10^{-12}$
K_{T3D}	$2,4328 * 10^{-8}$	K_{T3R}	$-1.1928 * 10^{-8}$
K_{T4D}	$-1,8243 * 10^{-5}$	K_{T4R}	$1.0508 * 10^{-5}$
K_{T5D}	0,0141	K_{T5R}	0.0057
K_{T6D}	0,0264	K_{T6R}	0.0020

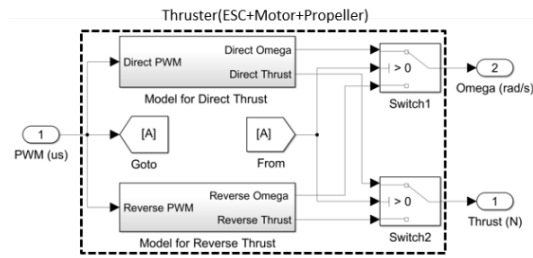


Figure 8. Simulink block of the final thruster model

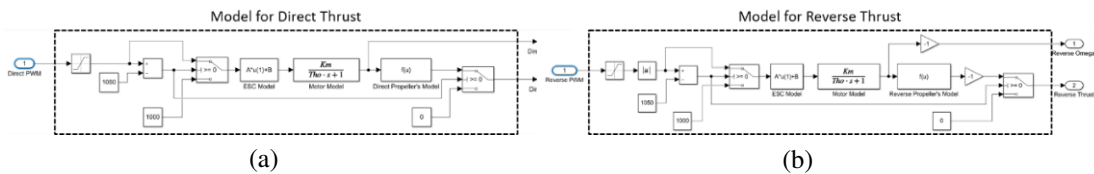


Figure 9. Simulink block for (a) direct and (b) reverse thrust model

3.3. Discussion

The response of the model simulated in open loop is shown in the Figure 10. The input is a PWM Sinus Wave and the output is the thrust force. We notice that the simulated system behaves like the real system, with the presence of a dead zone and a saturation zone. The Figure 11 shows the two responses of the thruster resulting from the experimental and simulation of the model obtained, we note that they have the same scale and that are almost identical. On the Table 3 are mentioned the means and quadratic errors between measurement and simulation values, we note that the errors are less than zero and this means that the simulation model reflects the real behavior of the thruster identified.

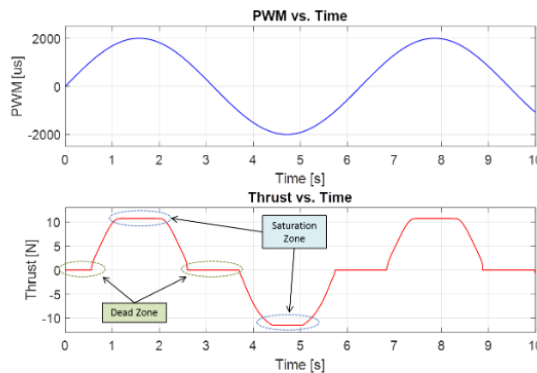


Figure 10. Thruster's model open loop response

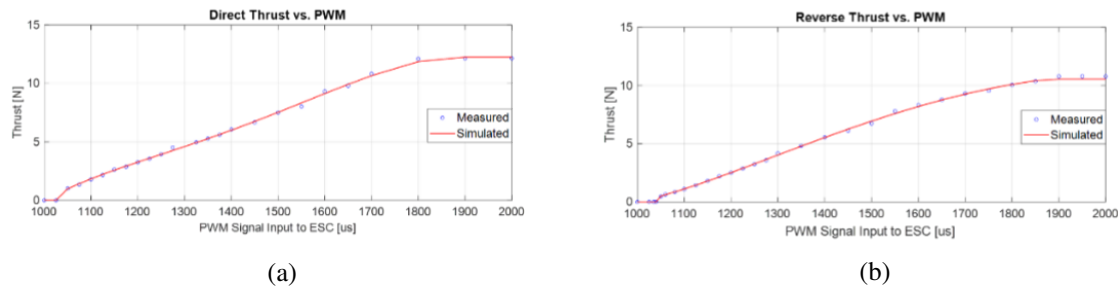


Figure 11. Simulation vs. experimentation thrust response for (a) direct and (b) reverse direction

Table 3. Simulation vs. experimentation thrust error comparison

	ME [N]	RMSE [N]
Direct thrust	0.0842	0.1184
Reverse thrust	0.0717	0.1083

4. IMPLEMENTATION ON UUV SIMULATOR

In this section we will use the UUV simulator to implement the model of the thruster identified above on an underwater vehicle, the aim is to test its performances to driving this last. The UUV simulator is a package containing the implementation of Gazebo plugins and ROS nodes necessary for the simulation of ROVs and AUVs [21].

As explained in [22] and shown in the Figure 12, the thruster model is implemented as two generic blocks that represent the dynamic model and the steady-state curve. They are 4 dynamics models available in the thruster plugin, including zero-order model, first-order model, Yoerger's model proposed in [23] and Bessa's extended model published in [24]. The Steady-State curve can be modeled as a constant gain like in (4), as constant gain with a dead-zone and as linear interpolation between input and output data that can be obtained from manufacturer's datasheet or from real test by a bench.

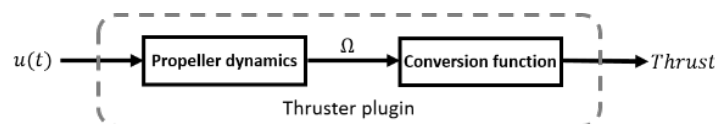


Figure 12. Thruster model plugin in UUV simulator

The first step is to take an existing ROV and replace their thrusters model by the ours, on the second step we make tests on the ROV with the new thruster model and show its behaviors and thruster's curves. The ROV that we have chosen is under development in our research laboratory (Figure 13), it has 6 thrusters mounted as follow:

- 4 thrusters in the horizontal plan, that make the ROV moves in the longitudinal X axis, Y axis and around the Z axis (Yaw movement).
- 2 thruster in the vertical plan, that make the ROV moves along the Z axis to allow the immersion.

The Figure 14 shows the packages and files that have been modified to integrate the characteristics of our thruster. The dynamics block is implemented as first order transfer function with a time constant equal to 0.01 s, and the conversion block as a polynomial with linear interpolation.

To start the tests on UUV simulator we followed the steps shown in the Figure 15, after the ROV is spawned we launch the dynamic positioning control by running: "roslaunch myrov_dp_controller start_myrov_dp_controller.launch" and the ROV begin tracking the desired waypoints. This node is based on a conventional proportional-integral (PI) controllers for 4 degrees of freedom (surge, sway, heave and yaw).

By running roslaunch service all the topics will be saved on a rosbag file, and exporting this file on MATLAB and using ROS toolbox [25], we can trace all what we need to show like positions, velocities and

sensors plugged in. The trajectory that will be tracked by the ROV is: diving 2 m, make a square of 10x10 m and return to the surface, as shown in Figure 16.

Figures 17-20 shows the corresponding responses to linear positions and velocities on X, Y and Z axes, and thrust forces generated. We notice that the forces generated by thruster to make move the ROV with the surge velocity of 0,5 m/s are around 2 N, but when turning, some thrusters delivering the maximum and minimum output forces of 12 N and -11 N respectively. The curves show a very good behavior of the ROV with the model of thruster described before. The Table 4 resume the main performances of the ROV using the thruster identified previously.

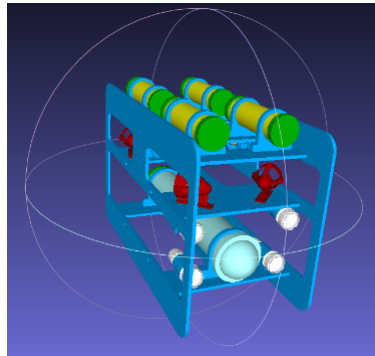


Figure 13. The ROV under development by AVCIS-lab

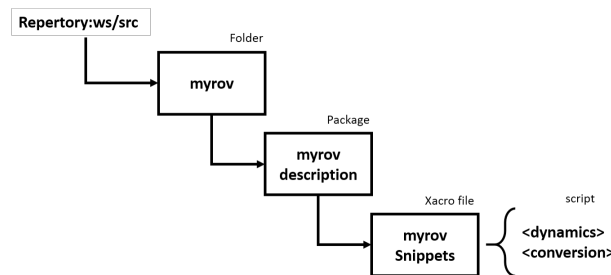


Figure 14. Implementation's diagram of thruster's model on our ROV package

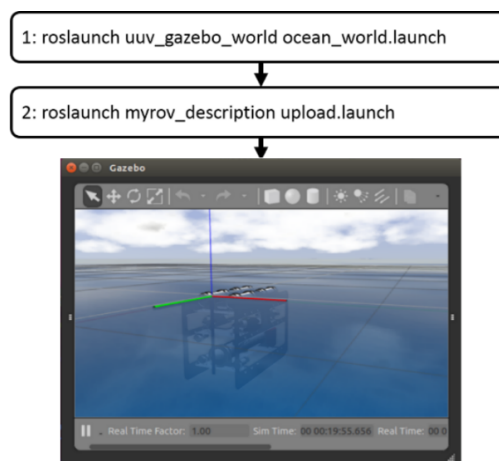


Figure 15. Steps to follow for starting tests on the ROV under UUV simulator

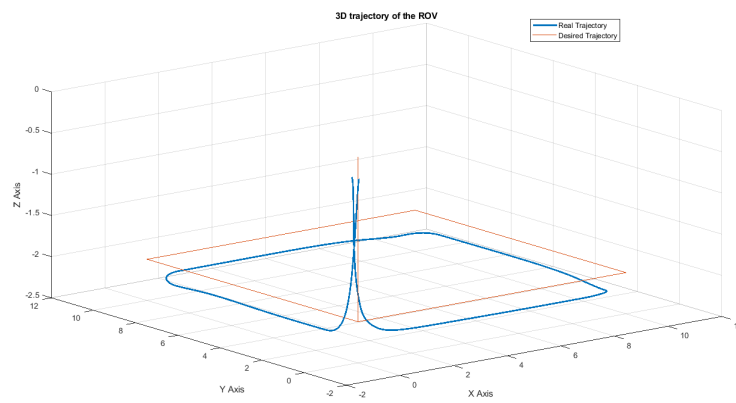


Figure 16. Tracked trajectory by the AVCIS-lab ROV

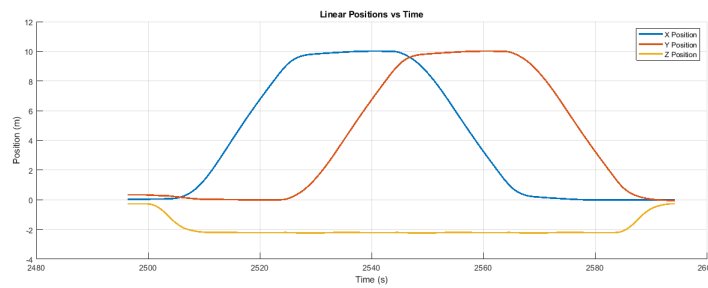


Figure 17. Linear positions of the ROV during trajectory tracking

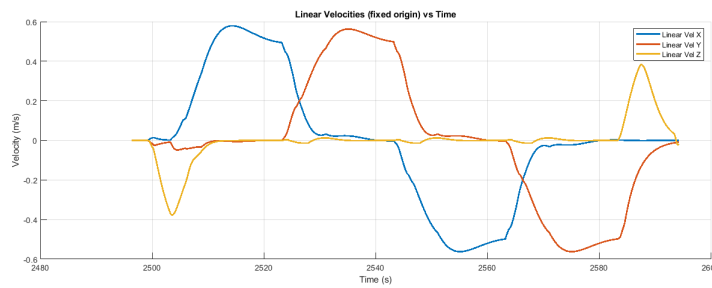


Figure 18. Linear velocities of the ROV during trajectory tracking

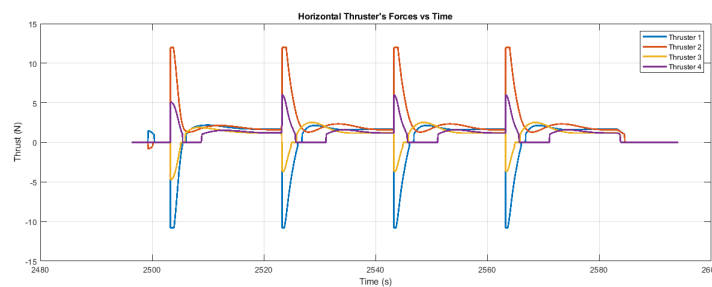


Figure 19. The thrust forces generated by the thrusters situated in the horizontal plan

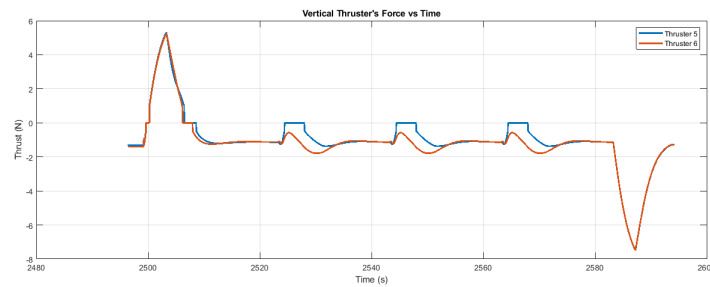


Figure 20. The thrust forces generated by the thrusters situated in the vertical plan

Table 4. Performances of the ROV with our thrusters

The ROV with our thruster	
Max forward velocity	2.8 m/s
Max backward velocity	-2.6 m/s
Max diving velocity	0.8 m/s
Max climbing velocity	-0.6 m/s
CW/CCZ yaw velocity	+/-1.1 rad/s

5. CONCLUSION

The thruster that we have identified is designed and constructed by our research laboratory using a 3D printing technology. The identification method used consisted of hybridizing between experimentation and simulation. In the experimentation part, we take into consideration the full thruster model in order to obtain the thrust characteristic as a function of the duty cycle input. In the simulation part, we take into consideration the model based only on the driver and the motor. The last step consists on deducing the model allowing the transition from the angular velocity to the thrust force. The model of the thrust force obtained as a function of the angular velocity is linear, contrary to what is already verified in the literature, this can be due to several factors: model of the motor used, the shape of the propeller fairing as well as the type of the propeller. A simulations in the open loop was made to show the behavior of the model obtained. In the last section we have used UUV simulator to mount the thruster's model on our ROV (under development) in the aim to show behavior by tracking a square trajectory with fixed forward velocity, the obtained outcomes are satisfactory.




REFERENCES

- [1] C. Guibert, E. Foulon, N. Ait-Ahmed, and L. Loron, "Thrust control of electric marine thrusters," *31st Annual Conference of IEEE Industrial Electronics Society, 2005. IECON 2005.*, 2005, pp.321-326, doi: 10.1109/IECON.2005.1568924.
- [2] J. Boehm, E. Berkenpas, C. Shepard, and D. A. Paley, "Tracking performance of model-based thruster control of a remotely operated underwater vehicle," *IEEE Journal of Oceanic Engineering*, vol. 46, no. 2, pp. 389-401, April 2021, doi: 10.1109/JOE.2020.2986593, 2020.
- [3] N.-H. Tran, Q. T.-D. Tran, N.-D. Nguyen, and H.-S. Choi, "Study on design, analysis and control an underwater thruster for unmanned underwater vehicle (UUV)," *International Conference on Advanced Engineering Theory and Applications*, 2017, pp. 753-764, doi: 10.1007/978-3-319-69814-4_73.
- [4] M. S. M. Aras, S. S. Abdullah, A. A. Rahman, and M. A. A. Aziz, "Thruster modelling for underwater vehicle using system identification method," *International Journal of Advanced Robotic Systems*, vol. 10, no. 5, p. 252, 2013, doi: 10.5772/56432.
- [5] A. Leonessa and R. Poirrier, "Adaptive control of marine thrusters," *MTS/IEEE Oceans 2001. An Ocean Odyssey. Conference Proceedings (IEEE Cat. No. 01CH37295)*, 2001, pp. 474-481 vol.1, doi: 10.1109/OCEANS.2001.968770.
- [6] Ø. N. Smogeli, A. J. Sørensen, and T. I. Fossen, "Design of a hybrid power/torque thruster controller with loss estimation," *IFAC Proceedings Volumes*, vol. 37, no. 10, pp. 409-414, 2004, doi: 10.1016/S1474-6670(17)31766-4.
- [7] J. Boehm, E. Berkenpas, B. Henning, M. Rodriguez, C. Shepard, and A. Turchik, "Characterization, modeling, and simulation of an rov thruster using a six degree-of-freedom load cell," *OCEANS 2018 MTS/IEEE Charleston*, 2018, pp. 1-7, doi: 10.1109/OCEANS.2018.8604897.
- [8] R. Yang, B. Clement, A. Mansour, M. Li, and N. Wu, "Modeling of a complex-shaped underwater vehicle for robust control scheme," *Journal of Intelligent & Robotic Systems*, vol. 80, no. 3, pp. 491-506, 2015, doi: 10.1007/s10846-015-0186-2.
- [9] K. Muljowidodo, S. Adi N, N. Prayogo, and A. Budiyo, "Design and testing of underwater thruster for SHRIMP ROV-ITB," *Indian Journal of Marine Sciences*, vol. 38, no. 3, pp. 338-345, 2009.
- [10] L. Deniellou, Y. Gallou, P. Gourmelen, and N. Seube, "Force control of underwater thrusters with application to auv motion control," *IEEE Oceanic Engineering Society. OCEANS'98. Conference Proceedings (Cat. No. 98CH36259)*, 1998, pp. 1054-1058 vol.2, doi: 10.1109/OCEANS.1998.724397.
- [11] W. Wang and C. M. Clark, "Modeling and simulation of the videoray pro iii underwater vehicle," *OCEANS 2006-Asia Pacific*, 2006, pp. 1-7, doi: 10.1109/OCEANSAP.2006.4393862.




- [12] L. Pivano, "Thrust estimation and control of marine propellers in four-quadrant operations," Ph.D. dissertation, Department of Engineering Cybernetics, Norwegian University of Science and Technology (NTNU), 2008.
- [13] B. Ropars, L. Lapierre, A. Lasbouygues, D. Andreu, and R. Zapata, "Redundant actuation system of an underwater vehicle," *Ocean Engineering*, vol. 151, pp. 276-289, 2018, doi: 10.1016/j.oceaneng.2017.12.025.
- [14] C. Guibert, "Modélisation et commande en poussée de moteurs à courants alternatifs en propulsion navale," Ph.D. dissertation, Université de Nantes, 2005.
- [15] A. Laidani, M. Bouhamida, M. Benghanem, K. Sammut, and B. Clement, "A low-cost test bench for underwater thruster identification," *IFAC-PapersOnLine*, vol. 52, no. 21, pp. 254-259, 2019, doi: 10.1016/j.ifacol.2019.12.316.
- [16] M. F. da Silva, F. F. Bastos, D. S. da Silva Casillo, and L. A. Casillo, "Parameters identification and analysis of brushless direct current motors," *IEEE Latin America Transactions*, vol. 14, no. 7, pp. 3138-3143, 2016, doi: 10.1109/TLA.2016.7587613.
- [17] F. Y. Cevher, "Autopilot and guidance design for a mini ROV (remotely operated underwater vehicle)," M.S thesis, Middle East Technical University, 2012.
- [18] L. L. Whitcomb and D. R. Yoerger, "Development, comparison, and preliminary experimental validation of nonlinear dynamic thruster models," *IEEE journal of oceanic engineering*, vol. 24, no. 4, pp. 481-494, 1999, doi: 10.1109/48.809270.
- [19] N. Aït-Ahmed, M. Vonnet, L. Loron, and C. Guibert, "On modeling of marine thrusters for underwater vehicles," *IFAC Proceedings Volumes*, vol. 40, no. 17, pp. 211-216, 2007, doi: 10.3182/20070919-3-HR-3904.00038.
- [20] L. V. Steenson, A. B. Phillips, E. Rogers, M. E. Furlong, and S. R. Turnock, "Control of an AUV from thruster actuated hover to control surface actuated flight," in *Specialists Meeting AVT-189/RSM-028, Assessment of Stability and Control Prediction, Methods for NATO Air & Sea Vehicles*, 2011, pp 1-13.
- [21] M. M. M. Manhães, S. A. Scherer, M. Voss, L. R. Douat, and T. Rauschenbach, "UUV simulator: a gazebo-based package for underwater intervention and multi-robot simulation," in *OCEANS 2016 MTS/IEEE Monterey*, 2016, pp. 1-8, doi: 10.1109/OCEANS.2016.7761080.
- [22] M. M. M. Manhães, "Unmanned underwater vehicle simulator documentation," Accessed Jul. 03, 2019. [Online]. Available: <https://uuvsimulator.github.io/>.
- [23] D. R. Yoerger, J. G. Cooke, and J.-J. Slotine, "The influence of thruster dynamics on underwater vehicle behavior and their incorporation into control system design," *IEEE Journal of Oceanic Engineering*, vol. 15, no. 3, pp. 167-178, July 1990, doi: 10.1109/48.107145.
- [24] W. M. Bessa, M. S. Dutra, and E. Kreuzer, "Thruster dynamics compensation for the positioning of underwater robotic vehicles through a fuzzy sliding mode based approach," *COBEM-18th International Congress of Mechanical Engineering, Ouro Preto (Brasil)*, 2005, pp. 605-612.
- [25] MathWorks, *ROS toolbox: user's guide (R2021b)*, The MathWorks, Inc.

BIOGRAPHIES OF AUTHORS






Abdelmalek Laidani    received the Engineer degree in Automation in 2009 from University of Sciences and Technology of Oran (USTO) and Master degree (Magistère) in Automatics control 2013 from the same university. Currently he is PhD student in Electrical Engineering Department at USTO and lecturer at the same department. His research interests are in underwater vehicles design, modelling and control. He can be contacted at email: abdelmalek.laidani@univ-usto.dz.



Mohamed Bouhamida    received the Engineer degree in Electronics 1982, the Magister degree 1992 and Doctorat d'Etat (Ph.D.) degree in Automatics, 2006 from the University of Sciences and Technology of Oran "Mohamed Boudiaf" (USTO), Algeria. After graduation, he joined the Automatic Department of USTO. He was a Professor, and director of Automatique Laboratory (AVCIS) at the same University. His research interests include electric machine drives, power electronics and process control. He can be contacted at email: m_bouhamida@yahoo.fr



Zakaria Bellahcene    Graduated as an engineer in Automatic from the University of (USTO), Oran. His main fields of interest are intelligent control design, robust nonlinear control applied to non linear systems. He is now a teacher in the department of Electrical and Control Engineering at USTO. He can be contacted at email: zakaria.bellahcene@univ-usto.dz.